THE ASTRONOMICAL JOURNAL VOLUME 74, NUMBER 8 OCTOBER 1969

An Analysis of the Mariner-4 Cratering Statistics

C. R. CHAPMAN
Department of Meteorology, Massachusetts Institute of Technology, Cambridge, Massachusetts

AND

J. B. POLLACK* AND CARL SAGAN*
Smithsonian Astrophysical Observatory and Harvard University, Cambridge, Massachusetts

(Received 16 May 1968; revised 10 June 1969)

A catalogue of craters and crater-like objects has been prepared from several sets of contrast-enhanced high-quality positive transparencies of the Mariner-4 photography. Craters were identified and counted by the same procedures used in the compilation of lunar crater catalogues; particular attention was given to crater class and quality. Counts of craters with diameters $D<20$ km begin to show the effects of incompleteness. Substantial erosion and obliteration of all but the largest craters has occurred during the history of Mars. The epochs of crater formation and crater erosion appear to be closely tied together in time. A statistical curve-fitting program for the observed crater diameter–frequency relations and a differential number–density distribution law of AD^{-B} give $B=2.5\pm0.2$ for $D>20$ km, or $B=3.0\pm0.2$ for $D>30$ km. The population of impacting objects assumed responsible for these craters is taken as having a differential number density varying as $X^{-\beta}$, where X is the diameter of the impacting object. The number of "live" comets and Apollo objects crossing the orbit of Mars is insufficient by more than 2 orders of magnitude to explain the observed number density of craters on Mars. For asteroidal objects with $\beta=2$ or 3, the predicted and observed number densities cannot be brought into agreement unless we assume an early epoch of very high cratering rates on Mars. For $\beta=4$ or 5, agreement between the predicted and observed number densities can be secured with a nearly uniform rate of asteroidal bombardment. For all reasonable values of β, impact damage contributes to crater erosion and obliteration, and asteroidal bombardment is capable of accounting quantitatively for the observed values of both A and B, particularly if the zone of obliteration around Martian craters is larger than that for lunar craters. For *near*-saturation bombardment, the existing observations are of very little use in determining the value of β, or in distinguishing between saturation bombardment and other erosion mechanisms. The dust produced by impact during the history of Mars is estimated to have depths between 0.1 and several km. For $\beta<3$, the mean ages of Martian craters are found to be approximately equal to the age of the planet. However, for β significantly larger than 3, different craters will have different mean ages, ranging down to $\lesssim 10^7$ yr for craters smaller than 20 km. Thus, the absence of such signs of running water as river valleys in the Mariner-4 photography is quite irrelevant to the question of the existence of bodies of water in early Martian history.

I. INTRODUCTION

ON 15 July 1965 (U.T.), the United States spacecraft Mariner 4 obtained, from a distance ~15 000 km, a sequence of 22 photographs of the surface of Mars. A preliminary discussion of the first 15 frames (frames 16–22 lacked usable contrast) was made by the experimenters Leighton, Murray, Sharp, Allen, and Sloan (1965) with particular emphasis laid on the statistics of the craters discovered in this pioneering mission. Their report was criticized and further discussed by others in a series of short reports (Anders and Arnold 1965; Baldwin 1965; Witting, Narin, and Stone 1965; Öpik 1965, 1966; Binder 1966; Hartmann 1966). Subsequent to the appearance of the final report of the Mariner-4 imaging experiment (Leighton, Murray, Sharp, Allen, and Sloan 1967), further short reports by Marcus (1968) and by Binder (1969) have appeared. We present here a new reduction of the photographic data with applications to the origin, age, and history of the craters, based in part on the discussion of Chapman, Pollack, and Sagan (1968; henceforth, Paper I).

* Now at Laboratory for Planetary Studies, CRSR, Cornell University, Ithaca, New York.

II. A NEW REDUCTION OF THE CRATERING STATISTICS

Three basic sources were employed for the Mariner-4 photography: (1) several sets of 8.5×11-inch glossy prints of the digital-to-analog conversion kindly provided by the experimenters and the Jet Propulsion Laboratory; (2) a set of high-quality 3.5×3.5-inch positive transparencies of the same bit conversion prepared at the Jet Propulsion Laboratory and provided through the kindness of Dr. James Edson; and (3) a set of high-contrast positive transparencies prepared photographically by Charles Hanson of the Smithsonian Astrophysical Observatory from set 2.

These sources were then used to compile a crater catalogue. The preparation of such a catalogue is a nontrivial task. The recent history of lunar crater studies provides several examples of incomplete or inexact crater counts leading to erroneous conclusions. In the case of the Mariner photographs, the difficulties are augmented by the poorer photographic quality, the generally small solar zenith angles, and problems in the connection of the photometric response of the video system for adjacent frames. One of us (CRC) has had experience in measuring and classifying lunar craters

TABLE I. Parameters of pictures 2–15 of the Mariner-4 photography.

Picture	Dimensions (km) E–W	N–S	Area (km²)	Filter	Solar altitude	Quality	km/line
2	470	850	398 000	green	70°	fair	5.2
3	350	500	177 000	green	76°	fair	3.1
4	340	430	147 000	orange	76°	fair	2.7
5	310	350	108 000	orange	71°	fair	2.1
6	310	320	99 000	green	68°	fair	2.0
7	290	290	84 000	green	51°	very good	1.8
8	290	270	80 000	orange	58°	good	1.7
9	270	260	70 000	orange	52°	good	1.6
10	270	260	70 000	green	49°	good	1.6
11	270	240	66 000	green	43°	very good	1.5
12	270	240	66 000	orange	40°	fair	1.5
13	270	230	62 000	orange	33°	fair	1.4
14	270	230	62 000	green	30°	fair	1.4
15	290	230	65 000	green	24°	fair	1.4

(Arthur, Agnieray, Horvath, Wood, and Chapman 1963, 1964) and is primarily responsible for compiling the catalogue of Martian craters (and possible craters) presented in the Appendix. The other two authors have checked these identifications. There is always the danger in such a catalogue that spurious craters may be listed, but a catalogue that includes only the entirely unambiguous features can be very misrepresentative—especially in the present case of small solar zenith angles, relatively poor contrast discrimination, and heavily eroded craters. Thus, while we have included a feature only when there appears to be good indication from several lines of evidence that it is indeed a crater (such criteria as circularity and appropriate illumination were weighted heavily), there may be several objects listed that are not true craters. The column of the catalogue headed "quality" distinguishes unambiguous from ambiguous craters. For all of the analyses based on this catalogue, the doubtful objects will be ignored. Although the best frames have a ground resolution of under 4 km, there are relatively few entries in the catalogue with diameters <10 km, owing to the poor quality and poor visibility of the smaller craters. However, close inspection of the best transparencies gives the distinct impression of many small craters slightly larger than the limiting resolution (a few scan lines across). Representative diagrams, showing the approximate positions and qualities of craters in selected frames are displayed in Paper I.

Table I summarizes the relevant parameters for each usable frame. The photographic-quality entry is a subjective measure of the clarity of a given picture, assuming that the region of the Martian surface in question has a well-defined intrinsic contrast. Among possible reasons for a variation in quality from frame to frame are the solar-illumination angle, the photometric-function program of the video system, surface erosion, and overlying clouds. A. Dollfus (1965, private communication) reports obscuration by white clouds of the region of pictures 12–15 a few days before encounter. The resolution is displayed in Table I as kilometers per line—the surface displacement corresponding to the video line separation. For pictures of "very good" quality, the catalogue is probably complete down to craters a few resolution elements across, at least for the less eroded craters. Considerable loss in completeness—particularly for craters of small diameter—can be expected for pictures where the quality is only "fair." Rounded-off estimates of the dimensions and areas of the Martian surface regions viewed in each picture, and the color filter used, are also displayed in Table I.

The catalogue in the Appendix presents all clear craters, and many additional ambiguous craterlike objects on pictures 7–14. The reliability of crater identification is much higher for 7–14 than for other frames. A sequence number, 1–298, was assigned to each crater (Paper I). After iteration in compiling the catalogue, a few entries have been dropped upon closer scrutiny; as a result, some sequence numbers (e.g., 124) do not correspond to probable craters. When a crater appears in the overlap region of two adjacent frames, separate values are listed under the same sequence number; in later data reduction such craters are counted only once. The approximate positions of craters in the catalogue are distances in centimeters from the south and west edges of the 8.5×11-inch prints distributed by NASA, and are intended for orientation of the reader interested in comparing his prints with the catalogue. Crater diameters displayed were measured in the unforeshortened direction and are uncertain to a few kilometers.

There are uncertainties in the reliability of identification of features from frame to frame, and within a given frame. A qualitative measure of this reliability is a parameter we call *crater quality*, to be distinguished from the picture quality of Table I. Factors affecting crater quality include picture quality, solar zenith angle, crater diameter, and crater class (see below). Quality A objects are definitely craters. Quality B objects are definitely Martian surface features, and are probably craters. Quality C objects may be craters. Some more-or-less circular features were omitted because of positive identification as photographic defects, or because the lighting was not that expected for a crater with the known solar illumination. Because of the relative clarity of lunar photography, it is not customary to introduce a crater-quality parameter in lunar studies. The analysis on the following pages is based only on craters of Quality A and B in pictures 7–14; these craters are in good agreement with those tabulated by Leighton *et al.* (1967). The comparison of the different crater tabulations is discussed by Binder (1969) and by ourselves (Chapman, Pollack, and Sagan 1969).

To be distinguished from crater quality is a parameter called *crater class*, which is customarily employed in lunar studies. The classifications 1–4 are an index of

crater morphology. For Martian craters we find (as for lunar and terrestrial craters) a continuous spectrum of crater forms, varying from fresh, sharp, circular, deep craters with concave floors and raised rims (class 1) to features so severely deformed or eroded as to be barely recognizable as craters (class 4). If large-scale Martian craters are produced by hypervelocity impact of asteroidal and cometary debris, then they must have all begun as class 1 craters, subsequently undergoing processes of deformation and erosion leading to craters of higher class. Similar classification schemes are widely used in lunar studies (Young 1940; Baldwin 1963; Arthur *et al.* 1963, 1964; Arthur *et al.* 1965; Arthur, Pellicori, and Wood 1966; Hartmann 1965), and have proved useful despite the differences among classification schemes.

The four classes employed in the present study are defined as follows:

Class 1: These fresh, uneroded craters are characterized by a prominent raised circular rim, a concave floor, and no appreciable softening or overlapping by other craters.

Class 2: These craters are somewhat less perfect and prominent than those of class 1. They have complete, relatively high walls, although some degree of softening and slumping may be evident. The central portion of the floors may be flattened, although much of the interior of these craters remains bowl-shaped. There may be some overlapping by small craters.

Class 3: These craters have flat floors. The walls are considerably lower in proportion to crater diameter than for classes 1 and 2, but they are still quite apparent and more-or-less complete. The craters may show some departure from circularity and may be overlapped. Their features may appear somewhat softened.

Class 4: These craters have very low walls, often with large portions barely distinguishable or missing. The floors are entirely flat. The craters may show considerable departures from circularity and are very battered and eroded, marked by much softening of detail, filling, and overlapping.

This classification is comparable to that of Arthur *et al.* (1963, 1964, 1965, 1966), with the exception that class 5 is omitted here. This class includes craters so severely destroyed as to be marginally visible, even on the best lunar photographs taken at large solar zenith angles. Similar Martian craters—in the few instances that they are detectable—are included as class 4 objects in the present catalogue. With this exception, the present classification should be quite comparable with that of Arthur *et al.* In classifying Martian craters, comparison was made with lunar craters on photographs with similar solar zenith angles. The same standards, based on the distribution of brightness over the crater, were used to determine Martian crater characteristics as are routinely used in lunar studies. One of the principal applications of the catalogue, outlined below, is an analysis of erosion on the Martian surface. To treat this problem conservatively, craters were generally given the lowest classification consistent with their appearances—i.e., the effect of solar illumination was slightly overcompensated for.

TABLE II. Crater percentages by class at several diameter intervals for Mars and the moon.

Region	Class	Diameter interval (km) 5–10	10–15	15–20	20–30	30–60	>60
Mars:	1	38	11	14	4	4	0
pictures 7–14,	2	58	26	24	9	8	14
Quality *A*	3	2	43	29	46	43	43
and *B*	4	2	20	33	41	54	43
Lunar	1	18	17	14	7	1	4
highlands:	2	25	23	26	27	19	12
(selected pure	3	44	35	24	24	25	32
continental	4	13	25	36	42	55	52
regions)							

The classification scheme presented here should be largely independent of such factors as crater diameter and solar zenith angle; the vast majority of classifications fall on a *relative* scale that should be duplicated by any independent classifier attempting to follow the class definitions above. In making the *absolute* classifications, we have assumed that the prevailing Martian terrain is not very rugged, consistent with the low general slopes deduced from radar Doppler spectroscopy (Sagan, Pollack, and Goldstein 1967). Some craters were not classified on the early frames because of difficulties introduced by the high altitude of the sun.

After completion of the catalogue and analysis of the present paper, a preliminary announcement was made of the production of electronically dodged, contrast-enhanced Mariner-4 frames, prepared by the experimenter team (Leighton *et al.* 1967). The total number of fairly unambiguous craters detected on the new frames is about 300, very close to the number of craters we report (Appendix and Paper I). For this reason, and for reasons discussed above and below, we believe that the analysis of the present paper does not require significant modification because of the new photographic reduction.

III. CRATER EROSION AND OBLITERATION

We assume that the large detectable Martian craters are of impact origin, as is generally believed to be true for lunar craters of comparable size.

An inspection of the crater catalogue (Appendix) reveals that a significant fraction of the craters belongs to classes 3 and 4. Of the 53 quality-A and -B craters on pictures 7 through 14 with diameters larger than 20 km, 87% are members of class 3 or 4. Since all impact craters would initially belong to class 1, we conclude

TABLE III. Minimum diameters for obliteration and equilibrium class membership.

α	$D^*_{\min}$	$D'_{3\min}$ (km)	$D'_{2\min}$
2	75	103	200
1	62	117	477
$\frac{1}{2}$	43	152	2540
$\frac{1}{4}$	21	263	73 000

that many craters have been significantly modified or eroded since their time of formation; they have been largely filled in, and in some cases their ramparts have been breached.

It is natural to ask at this point whether some craters have been so severely damaged as to be indetectable on the Mariner-4 photographs. An inspection of Crater 217 of picture 11 suggests that some of the smaller craters would be almost completely obliterated. If a crater 150 km in diameter can be significantly eroded (among other criteria, its western ramparts are entirely missing), then smaller craters of a similar or greater age may be entirely expunged. We wish to estimate the scale of the erosion process.

Presented in Table II are the fraction of craters in each class for several diameter intervals. Below about 20 km, the counts of the poorer-class craters are incomplete, a point to which we return shortly. For the diameter intervals above 20 km, the class percentages are remarkably similar. This suggests a common erosion history for craters of diameter larger than 20 km, and permits us to use the extensive erosion of the larger craters to infer obliteration of the smaller craters.

Suppose that the lifetime of a crater of class i scales as D^α, where α may be either zero or positive, its value depending upon the mechanisms of erosion. Let D^* represent the diameter of the largest crater which has been obliterated by the erosion processes. All larger craters ever formed will still be present and larger diameters will have smaller percentages of poor-class craters. At diameters smaller than D^*, the crater population is in steady state with the erosional processes and the percentages of craters by class will be the same at all diameters. Thus we can derive $D^*_{\min}$, a lower bound to D^*, by finding the largest diameter for which we can be confident of our observation of the constancy of the percentages of craters in each class (Table II). Allowing for statistical fluctuations, we can assert that the fraction of class-4 craters at diameters over 60 km is at least half the fraction for the smaller craters. This condition is expressed mathematically in Paper I, and leads to the various estimates of $D^*_{\min}$ as a function of α shown in Table III. (Also shown are analogous lower bounds $D^*_{i\min}$ on the diameter at which equilibrium values are reached for class i craters.) Except for $\alpha=0$, all plausible erosional mechanisms can be expected to have $\alpha \geq 0.5$. Thus 43 km is a lower limit to D^*. In the case that $\alpha=0$, no bound can be placed; however, we will see below that for one expected $\alpha=0$ erosional process, obliteration of craters larger than 20 km does occur.

Another method for estimating D^* is to find a "knee" or break in the slope of the log–log diameter–frequency relation for the craters. If there is a *real* deficiency of craters at diameters below the knee (compared with an extrapolation of the frequency relation for larger craters), the diameter at the knee may be interpreted as D^*. Using this approach, Hartmann (1966), Binder (1966), and Öpik (1966), have claimed that obliteration sets in at about 50 km, 40 km, and 20 km, respectively. Hartmann's and Binder's results actually do not clearly indicate a deficiency except for craters with diameters below about 30 km. We believe that these deficiencies are *not* real and are in large part due to observational incompleteness in the crater counts. While the sharp class 1 objects can be observed down to such small diameters as a few kilometers, as limited by the resolution of the video system and the quality of the picture, the later-class craters will show incompleteness at larger diameters. Table II illustrates this point: Between 5 and 10 km, only 4% of the craters in the catalogue are of class 3 or 4. There seems to be some incompleteness up to at least 20 km. Since class-3 and -4 craters constitute a major fraction of the larger craters, their incompleteness at smaller diameters could easily lead to the effect found by Hartmann, Binder, and Öpik. Our own crater counts, based on many more craters than just the obvious ones counted by early investigators, yield a frequency relation which shows no obvious knee above the diameter where incompleteness sets in (see Fig. 1). On this point, our analysis agrees with the recent work of Marcus (1968).

Leighton, Murray, Sharp, Allen, and Sloan (1967), from a study of the Mariner-4 vidicon-response function and particularly from a study of plaster-of-paris models of craters photographed with the Mariner-4 system, deduce a real discontinuity at about 20 km. However, their crater models are of well-preserved (class 1 and 2) craters, not of the more poorly preserved craters that suffer incompleteness earlier. In examining the results of Leighton *et al.*, we find that a bend in the diameter–frequency curve begins at about 30 km or slightly larger diameters. We suspect that this difference is due in part to the inclusion by Leighton *et al.* of very poor quality craters. For these reasons and for the additional reasons mentioned above, we are not persuaded that a 20- or 30-km break is real.

The percentages of craters by class also permit us to make a rough comparison between the times of the last significant erosion and the last important epoch of crater formation. The existence of many badly damaged smaller craters implies that erosion continued until close to or after crater formation ended (or at least greatly slowed down). The presence of some craters of classes 1 and 2 shows that erosion could not have continued long

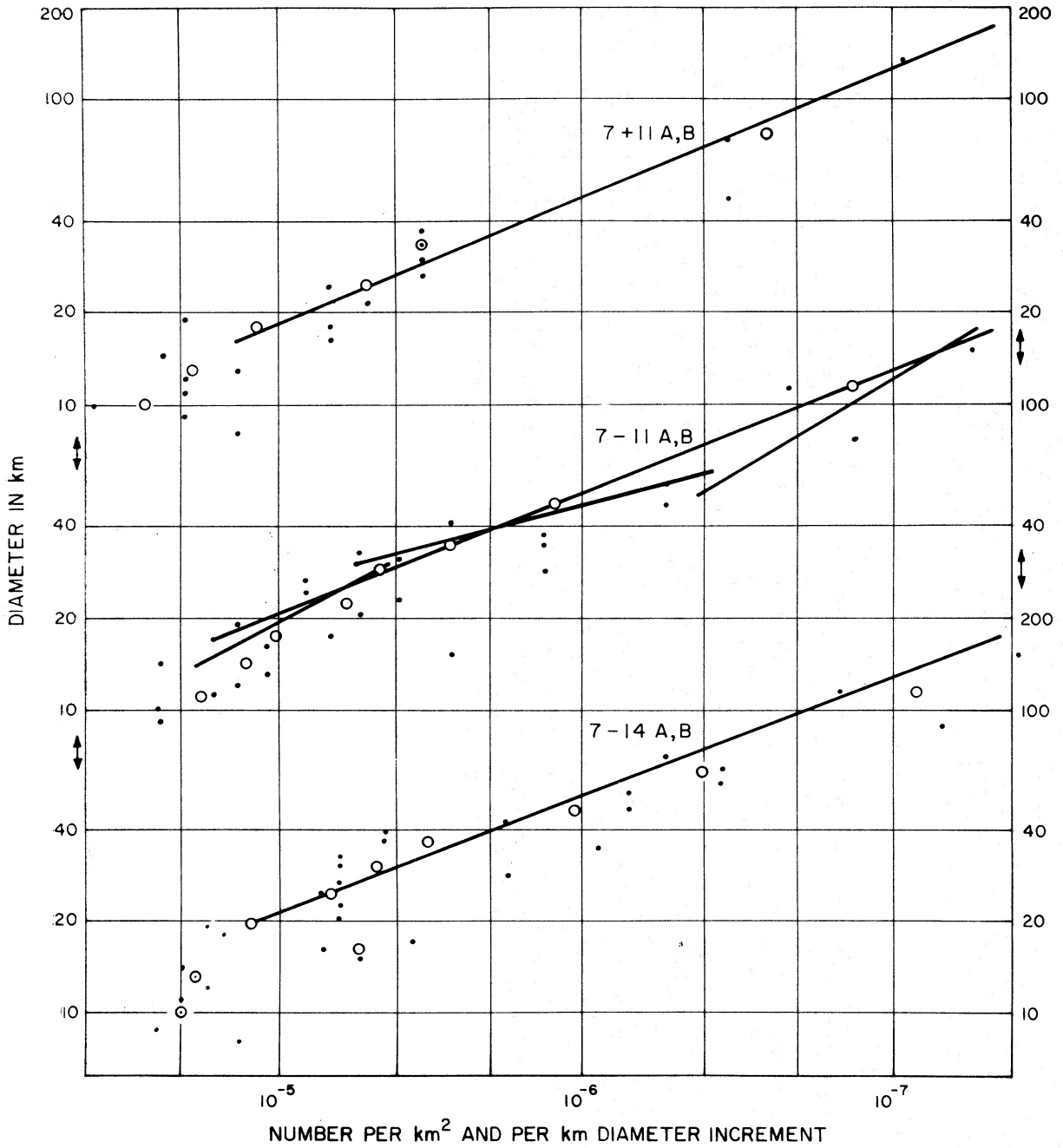

FIG. 1. Diameter–frequency plot for pictures 7–14, qualities *A* and *B* (*top*); pictures 7–11, qualities *A* and *B* (*center*); and pictures 7–11, qualities *A* and *B* (*bottom*). The dots are the original counts; the circles are these counts grouped by threes; the straight lines represent increment-weighted least-squares fits. The incompleteness of the crater counts for *D* less than 20 km is particularly evident for the *bottom* plot.

after the last period of bombardment. This conclusion is, of course, compatible with, although not uniquely indicative of, a uniform rate of crater formation and erosion, continuing to the present. It is also compatible with saturation bombardment as the principal crater-erosion mechanism.

In summary, many of the observed craters have been severely eroded, and except for one choice of α, complete obliteration of the oldest craters smaller than 43 km and perhaps some larger craters during the history of Mars is inferred. Crater formation and erosion appear to be closely tied together in time.

TABLE IV. Comparison of predicted and observed numbers of Martian craters.
(Predictions assume uniform bombardment rate.)

Source	β	ν	D_c	X_c	Predicted $N(X>X_c)$	Observed $N(D>D_c)$ Eq. (1)	Eq. (2)
Comets	···	3	12.8 km	1 km	$\leq 1.2\times10^{2}$	2.9×10^{4}	6.6×10^{4}
Comets	···	3.6	5.5	1	$\leq 1.2\times10^{2}$	9.3×10^{4}	3.6×10^{5}
Asteroids	2.5	3	20	0.62	7.5×10^{2}	1.35×10^{4}	2.7×10^{4}
Asteroids	2.5	3.6	20	1.55	1.9×10^{2}	1.35×10^{4}	2.7×10^{4}
Asteroids	4.5	3	20	0.62	3.2×10^{5}	1.35×10^{4}	2.7×10^{4}
Asteroids	4.5	3.6	20	1.55	1.3×10^{4}	1.35×10^{4}	2.7×10^{4}

IV. SOURCES OF IMPACT CRATERS

We will attempt to find the most abundant source of impacting objects and see to what extent it can account for the observed number of Martian craters.

Kuiper (1959), Öpik (1960), and others have suggested that some of the large lunar craters, particularly in the maria areas, can be attributed to cometary impact. Some of these comets are "dead" short-period comets consisting only of nuclei that have survived disintegration due to heating, outgassing, tidal interaction, etc. An upper limit on the number of such comets can be found by considering all members of the Apollo group to be "dead" comets. Apollo objects are the largest bodies known to cross the orbit of the Earth. Of the eight observed members, seven have diameters exceeding 1 km. Öpik (1963) points out that, owing to observational incompleteness, the actual number of Apollo members with a diameter in excess of 1 km may be about 40. Öpik also estimates from the observations that there may be twice as many "live" comets crossing the Earth's orbit with diameters in excess of 1 km. Many of these live comets may be destroyed in passing through a planetary atmosphere. Thus, an upper limit (and perhaps a generous one) to the number of Earth-crossing comets with diameters in excess of 1 km and capable of producing large craters is about 100. A similar figure will hold for the number of Mars-crossing comets; furthermore, this figure should be fairly constant with time.

A second source of impacting bodies on Mars is Mars-crossing asteroids which come from the asteroid belt located between the orbits of Mars and Jupiter. There are ten observed Mars-crossing asteroids with diameters larger than 20 km. The number of asteroids with diameters between X and $X+dX$, where $X>20$ km, is given approximately by a power-law dependence:

$$n(X)dX=200X^{-2}dX, \quad X \text{ in km}, \quad X>20 \text{ km}$$

(cf. Öpik 1963). For diameters smaller than 20 km, incompleteness sets in, and it is not necessarily valid to assume that $n(X)$ will continue to scale as X^{-2}. In extrapolating $n(X)$ as $X^{-\beta}$ from 20 km to 1 km, observational considerations suggest that β lies between 2 and 5 (Kuiper *et al.* 1958; Kuiper 1965) while theoretical considerations (Hawkins 1960; Dohnanyi 1969) suggest $3.5\leq\beta\leq4$.

We now estimate the number of craters expected from comets and asteroids using the well-known equations for the production of craters by impacting bodies (see, e.g., Baldwin 1963 and Paper I). In performing the calculations, we assume that the velocity of impact immediately before collision was 11.5 km/sec (Öpik 1963) and the density of the asteroidal bodies and cometary bodies was 7.8 gm/cm^3 and 1.3 gm/cm^3, respectively. Reasonable variations in these values will not affect our conclusions. Furthermore, we select ν, the exponent in the relationship between energy of impact and crater diameter, as lying between 3 and 3.6 (Shoemaker *et al.* 1961; Baldwin 1963) and the lifetime for asteroidal impact as 7.4×10^{9} yr and about half this figure for comets (Öpik 1963; see also Dohnanyi 1969). The latter figures are representative of the present population of these bodies. Such a value is probably valid for comets in the past, but may be an overestimate for the Mars-crossing asteroids, since asteroids with shorter lifetimes would no longer be present.

The observed differential diameter–frequency relation, $n(D)=AD^{-B}$, expresses the number of craters on Mars having diameters within a 1-km diameter increment centered on D. In order to determine the values of A and B from the data in our crater catalogue, we have used a statistical curve-fitting program written by Chapman and Haefner (1967) for analyzing lunar craters. The parameters A and B vary somewhat with crater diameter, crater class, and quality; but after extensive study, we have found that the crater sample is too small to allow reliable estimates of these variations. Much more refined statistical analyses will be possible if future photographic missions to Mars can obtain five-times better surface coverage with the same or improved resolution.

It is particularly crucial to determine the maximum diameter at which some observational incompleteness exists since the curve-fitting procedure heavily weights counts at smaller diameters. In general, we believe the crater sample is complete above 20 km, but we cannot rule out the possibility of some loss of class 4 craters between 20 and 30 km; hence, we will carry two diam-

eter–frequency relations as representing the observations (pictures 7–14, qualities A and B only):

$$A=2.0\times10^{6}\pm1.2\times10^{6},\ B=2.5\pm0.2 \text{ for } D>20 \text{ km}, \quad (1)$$

$$A=1.6\times10^{7}\pm1.3\times10^{7},\ B=3.0\pm0.2 \text{ for } D>30 \text{ km}, \quad (2)$$

in units where D is measured in kilometers. The errors represent one standard deviation. The observed diameter–frequency relationship is shown in Fig. 1. The discussion by Leighton *et al.* (1967) implies $B\simeq3.2$ for $D>30$ km, in good agreement with our results. Also Marcus (1968) obtained $B=3.0$.

For the moment we assume that all craters which have been produced are still visible and that the present collision rates equal the time-averaged values. Table IV compares the observed and predicted number of craters of size in excess of D_0 km, which are produced by bodies whose diameter is greater than X_0 km. Clearly the cometary supply is insufficient to explain the observed craters. If the population index of Mars-crossing asteroids, β, is sufficiently large, the Mars-crossing asteroids can supply enough craters without any necessity to invoke a higher bombardment rate in the past. But such large values of β can be compatible with the observed small value of the population index B for the craters only if a substantial number of craters have been obliterated. As a result, the predicted value overestimates the number of observable craters; in reality not enough craters are produced for cases where ν is appreciably greater than 3. In our calculations below we will assume ν equals 3.

Öpik (1966) performed similar calculations and found a discrepancy of a factor of about 5 between theory and observation for β close to 2.5. Our more complete crater count implies that there are about 50 times more craters observed than predicted, with β equal to 2.5 and a constant bombardment rate. Öpik suggested that this difficulty could be circumvented by postulating a higher bombardment rate in the past. For example, there may have been many planetesimals present in Mars-crossing orbits when Mars first formed, and most of these may have had low inclinations and semimajor axes similar to those of Mars, which would imply small collision lifetimes. Above we have pointed to a second option; β may be about 4.5.

With a value for ν of 3, and in the absence of obliteration, the population index B for the differential number of craters would equal β. But B is 2.5 ± 0.2 for craters larger than 20 km and 3 ± 0.2 for craters in excess of 30 km. Thus obliteration must be invoked if β has a large value. In fact to reconcile the excess of predicted craters in Table IV, obliteration would have to be invoked. We can again estimate D^* by equating the predicted number of craters larger than D^* with those observed to be larger than D^*. Table V summarizes these calculations. We see that for $4.0\leq\beta\leq5.0$, we obtain estimates of D^* consistent with substantial obliteration above 20 km (hence $B<\beta$) and with our earlier calculations of $D_{\min}{}^*$ (See Table III). Since α is given by $\beta-B$ (for $\nu=3$), the observed Martian crater distribution is consistent with crater production by asteroidal bombardment at a rate similar to the present rate and with crater erosion by a process for which $1\leq\alpha\leq2$.

TABLE V. Estimates of D^* from distribution functions.

$\beta=$		3.5	4.0	4.5	5.0
D^*(km)	Eq. (1)	20	56	95	131
	Eq. (2)	12	68	133	181

Note Added in Proof. D. Gault has suggested to us that, for craters of the size discussed in the present paper, the exponent in the relation between impact energy and crater diameter is $\nu\simeq4$. If this is correct, the present asteroidal bombardment rate is inadequate —even for large β—to account for the observed number of Martian craters (cf. Table IV); accordingly, most of the craters would have been produced in an early epoch of intense bombardment.

V. MAJOR TOPOGRAPHICAL FEATURES AS POSSIBLE CRATERS

Several large Martian bright areas, such as Elysium, Eridania, Hellas, and the Isidis Regio–Neith Regio complex, have a strikingly circular appearance, and it is natural to inquire whether these could be ultimately the results of impacts caused by very large asteroids. This suggestion is independent of the question whether such large circular bright areas are today highlands or lowlands. The bright areas of the sort mentioned have a diameter of 1000 km or more and would require an impacting object of diameter approximately 35 km or larger to create them. At present there are five Mars-crossing asteroids with diameters exceeding 35 km. Since the mean collision time with Mars is approximately equal to the lifetime of the planet (Öpik 1963), the present number of Mars-crossing asteroids is capable of explaining such features without the invocation of a higher bombardment rate in the past. This model is consistent with $\beta>3$. On the other hand, suppose we accept the suggestion of a very high initial bombardment rate with the exponent β equal to 2.5. Then Table IV implies that the predicted number of Martian craters must be raised by at least a factor of 20 over the number predicted with a uniform bombardment rate; thus, there should be over 100 craters with diameters exceeding 1000 km. Mars is certainly not saturation bombarded at such a resolution. If any other erosion mechanism were to remove most of the 100 craters with $D>1000$ km, it would be even more effective for smaller diameters where we should see no craters at all. Therefore, unless we wish to invoke histories that are very different for large asteroids than for small ones, these predictions based on $\beta=2.5$ seem contrary

TABLE VI. Predicted and observed number of craters on Mars, 20 km$\leq D \leq D^*$, $\beta > 3$.

β	$(\epsilon)^{\frac{1}{2}}=1$	$(\epsilon)^{\frac{1}{2}}=2$	$(\epsilon)^{\frac{1}{2}}=3$	Observed value
4	2.0×10^5	2.5×10^4	7.4×10^3	1.1×10^4
4.5	3.3×10^5	2.9×10^4	6.9×10^3	1.2×10^4
5	4.4×10^5	3.0×10^4	6.1×10^3	1.3×10^4

to observations; for this reason a more uniform bombardment rate with β substantially larger than 2.5 seems to be preferred. Were the dark areas of impact origin, the same conclusions would follow, since even fewer very large circular dark areas exist on Mars.

VI. EROSION MECHANISMS

In this section we discuss various mechanisms by which newly formed craters can be eroded and obliterated. The damage produced by impacting objects on nearby craters will be the first such process to be considered; it is readily susceptible to a quantitative treatment.

When a sufficient number of craters is produced, the probability becomes large that new craters will form on or near existing craters. If the size of the new crater is comparable to or larger than the old crater, and if the new crater is produced within the same area as the old one, it will clearly tend to obliterate the old crater. If the impacting object falls sufficiently close to, but not contiguous with, the old crater, it may still obliterate the old crater both by filling in the old crater with some of the debris created in the formation of the new crater and by the damage caused by surface shock waves generated by the new impact. Finally, when the old crater is far enough away from the center of the new crater not to be destroyed totally, it may nevertheless be sufficiently close to the new crater to suffer substantial damage. Similarly, new craters small in size compared to an old crater will not be able to destroy the preexisting crater, but they can damage it. Thus, in several ways, impacts are capable of causing erosion and obliteration of craters. In what follows we will try to distinguish carefully between obliteration of craters by subsequent impacts and erosion of craters by a similar mechanism.

In assessing the importance of impact damage we will compare predicted and observed slopes and numbers of craters under the assumptions that saturation bombardment conditions pertain. The relevant equilibrium equations are given in Paper I as well as in a report by Walker (1967). In obtaining numerical values we have selected 3000 km as the size of the largest crater, since we have seen in Sec. V that craters larger than 1000 km will form; however, a crater diameter in excess of the planet's radius is not expected.

We first compare population indices. When β is below 3, most of the obliteration is attributable to the largest craters and the equilibrium value of the population index equals β. Thus the case of β equal to 2.5 agrees with the observed values of the slope quoted above. However with β above 3 the craters comparable in size to the crater being obliterated are the most effective obliteration agents and the equilibrium population index becomes 3, again in reasonable agreement with the observations.

In computing the equilibrium number of craters we assume that a crater of diameter D will obliterate older craters lying within $\epsilon^{\frac{1}{2}}D/2$ of the center of the newly formed crater. The parameter $\epsilon^{\frac{1}{2}}$ will be on the order of unity but not necessarily exactly unity as secondary aspects of crater formation, such as shock waves, may abet obliteration. In performing the calculations for $\beta=2.5$, we underestimate the number of impacting bodies by assuming there to be just enough to account for the observed number of craters.

For β equal to 2.5, the observed and predicted number of craters agree quite well with $\epsilon^{\frac{1}{2}}$ close to unity. Table VI compares the number of craters between 20 and D^* km with the amounts predicted for large values of β and various choices of $\epsilon^{\frac{1}{2}}$. Agreement is secured when $\epsilon^{\frac{1}{2}}$ is close to 2. Thus, the two domains of β require different values of $\epsilon^{\frac{1}{2}}$ for impact damage to account for the observed number of craters. However it is not yet possible to tell which value of $\epsilon^{\frac{1}{2}}$ is more reasonable. If β equals 2.5, since $\epsilon^{\frac{1}{2}}$ cannot be less than 1, impact damage must be the dominant obliteration mechanism, i.e., the observed crater density is very close to the maximum allowable value. Thus some crater obliteration should have occurred by impact damage; furthermore, there can be no more effective obliteration agent. Its importance for the large values of β depends on what value $\epsilon^{\frac{1}{2}}$ assumes, but for any value it should make a significant contribution to obliteration.

For $\beta=2.5$, the time scale for obliteration for the observable craters is independent of diameter and so the index α equals zero, while for values of β between 4 and 5, α equals $(\beta-B)$ or 1 to 2.

Thus, we find that crater overlap and near-saturation bombardment as a mechanism for crater erosion and obliteration are susceptible to quantitative treatment and seem able to account for much of the damage sustained by the Martian craters. However, there are other possible contributing mechanisms to crater erosion during the history of Mars which cannot at the present time be excluded (Paper I): these include erosion due to windblown dust of impact or micrometeoritic origin, liquid water on large or microscales, and mountain building and flooding by lava.

VII. CRATERS AS SOURCES OF DUST

Polarimetric, photometric, and infrared radiometric studies have shown the Martian surface is covered with dust (cf. Pollack and Sagan 1967). Radar observations of the bright areas indicate that the dust extends down to a depth of at least a meter (Sagan and Pollack 1965).

One abundant source of such a large amount of dust is the cratering process; the hypervelocity impacts responsible for the craters pulverize and eject large amounts of material.

We now estimate the average depth $\langle S \rangle$ to which the currently observed craters have penetrated the Martian surface. We find $\langle S \rangle$ by dividing the volume produced by crater formation by the area of the planet (see Paper I). We assume that the depth of the crater is 1/20 of its diameter; $\langle S \rangle$ then lies between 0.1 km and several km for all values of β.

In either case, ejecta produced by impact could make major contributions to crater erosion. If even a very small fraction of the ejecta so produced is eventually converted into particles small enough to be moved by contemporary Martian winds, it will have a large enough volume to cover the bright areas to a depth of a meter, which is the lower limit placed by the radar observations. The cratering process is, therefore, a promising mechanism to account for the large quantities of dust present on Mars.

VIII. CRATER AGES

Much of the previous analysis of the Mariner-4 cratering statistics has been devoted to a determination of the "age" of the Martian surface; i.e., the time since the underlying features have been eroded away (Leighton *et al.* 1965; Anders and Arnold 1965; Baldwin 1965; Witting *et al.* 1965; Öpik 1965, 1966; Binder 1966; Hartmann 1966). These authors have generally made a comparison of the crater densities in the Mariner-4 region of Mars with those of the lunar maria. The age of the Martian surface then depends on an estimate of the relative bombardment rates, and a guess of the age of the lunar maria. With the maria assumed to be several billion years old, the Martian surface has been estimated to have ages ranging between 0.8×10^9–4.5×10^9 yr. An obvious uncertainty in this procedure is the estimate of the age of the lunar maria.

Within the context of the models of the present paper, we can obtain ages directly from the Martian crater counts, and independently of the age of the lunar maria. Such a procedure ultimately depends on estimates of the absolute bombardment rate on Mars. Models with $\beta<3$ require, as we have shown, a great flurry of crater formation in the early history of the planet; thus, almost all cratered areas would have an age comparable to that of Mars. For those models with $\beta>3$, a more uniform bombardment rate is implied; the largest craters, with $D>D^*$, will again have an age comparable to that of Mars, but the mean age of such craters will be half the age of Mars. As Hartmann (1966) has quite properly emphasized, the ages of craters with $D<D^*$ will be a function of D. A unique crater age for the Martian surface is an erroneous concept for $\beta>3$.

The lifetime of a crater smaller than diameter D^* will scale as D^α where α equals $\beta-B$. With this scaling law we have obtained the average ages of craters of various sizes, which is exhibited in Table VII.

TABLE VII. Mean ages of Martian craters (in units of billions of years).

		Diameter, D (km)				
	β	20	40	75	100	500
$\beta=B$	2.5 or 3.0	4.5	4.5	4.5	4.5	4.5
$\beta>B$	4.0	0.46	1.28	2.25	2.25	2.25
($B=2.5$)	4.5	0.094	0.64	1.32	2.25	2.25
	5.0	0.022	0.13	0.60	1.24	2.25
$\beta>B$	4.0	0.66	1.32	2.25	2.25	2.25
($B=3.0$)	4.5	0.13	0.37	0.95	1.46	2.25
	5.0	0.028	0.11	0.39	0.69	2.25

For the larger craters, the ages are compatible with those derived from assumptions on the ages of lunar maria. For smaller craters ($D=10$–25 km) and a uniform bombardment rate ($\beta>3$), the crater ages are tens to hundreds of millions of years; and for still smaller craters the ages are even less. Thus, Martian surface features with dimensions of 10 km or less will, for $\beta>3$, have ages much less than the age of the solar system. Accordingly, if substantial aqueous-erosion features—such as river valleys—were produced during earlier epochs on Mars, we should not expect any trace of them to be visible on the Mariner-4 photographs unless they were of greater extent than typical comparable features on Earth. Even if $\beta<3$, the same conclusion follows, because the dust produced by all causes during the subsequent history of the planet should easily be enough to fill such features (cf. Secs. VI and VII). Thus, any conclusion from the Mariner-4 photography that the apparent absence of clear signs of aqueous erosion excludes running water during the entire history of Mars—making the origin of life on primitive Mars unlikely—must certainly be regarded as fallacious.

IX. RECOMMENDATIONS FOR FUTURE WORK

From the conclusions and uncertainties of the present paper, it is clear that there is much room for further work in this subject. Laboratory and field work on the dependence of $\epsilon^{\frac{1}{3}}$ on soil type and on the dependence of incompleteness estimates on crater class is needed. Future space-vehicle missions could profitably photograph larger areas to obtain data on the largest craters, to search for relatively uncommon geological features on Mars, and to improve the cratering statistics with better resolution (to narrow the error in B—now hovering precipitously around the theoretically significant value of 3.0), and with a favorable range of solar zenith angles. A close flyby would of course be very useful in this regard, but an orbiter is what is really needed.

ACKNOWLEDGMENTS

We are indebted to Dr. James Edson for high-quality transparencies of the Mariner-4 digital-to-analog data

reduction; to Charles Hanson for preparing photographically contrast-enhanced transparencies of these data; to Dr. J. Focas and Dr. A. Dollfus for maps of the Mariner-4 encounter area drawn near encounter; and to Dr. E. Anders, Dr. G. Hawkins, Dr. G. P. Kuiper, Dr. R. B. Leighton, Dr. B. C. Murray, Dr. R. P. Sharp, and Dr. F. L. Whipple for helpful conversations. We are also grateful to Dr. Leighton for permitting us to examine an advance copy of the experimenters' final report (Leighton *et al.* 1967). This work was supported in part by NASA grant NGR 33-010-082 and NASA Contract 952487.

REFERENCES

Anders, E., and Arnold, J. R. 1965, *Science* **149**, 1494.
Arthur, D. W. G., Agnieray, A. P., Horvath, R. A., Wood, C. A., and Chapman, C. R. 1963, *Commun. Lunar Planet. Lab.* **2**, 71.
——. 1964, *ibid.* **3**, 1.
Arthur, D. W. G., Agnieray, A. P., Pellicori, R. H., Wood, C. A., and Weller, T. 1965, *ibid.*, 61.
Arthur, D. W. G., Pellicori, R. H., and Wood, C. A. 1966, *ibid.* **5**, No. 70.
Baldwin, R. B. 1963, *The Measure of the Moon* (University of Chicago Press, Chicago, Ill.).
——. 1965, *Science* **149**, 1498.
Binder, A. B. 1966, *ibid.* **152**, 1053.
——. 1969, *ibid.* **164**, 297.
Chapman, C. R., and Haefner, R. R. 1967, *J. Geophys. Res.* **72**, 549.
Chapman, C. R., Pollack, J. B., and Sagan, C. 1968, *Smithsonian Astrophys. Obs. Special Rept.*, No. 268 (Paper I).
——. 1969 (to be published).
Dohnanyi, J. S. 1969, *J. Geophys. Res.* **74**, 2531.
Hartmann, W. K. 1966, *Icarus* **5**, 565.
Hawkins, G. 1960, *Astron. J.* **65**, 318.
Kuiper, G. P. 1959, *Vistas in Astronautics* (Pergamon Press, Inc., New York, N. Y.), Vol. 2, p. 273.
Kuiper, G. P., Fugita, Y., Gehrels, T., Groeneveld, I., Kent, J., Van Biesbroeck, G., and Van Houten, C. J. 1958, *Astrophys. J. Suppl.* **3**, 289.
——. 1965 (private communication).
Leighton, R. B., Murray, B. C., Sharp, R. P., Allen, J. D., and Sloan, R. K. 1965, *Science* **149**, 627.
——. 1967, *JPL Tech. Rept.*, No. 32-884.
Marcus, A. H. 1968, *Science* **160**, 1333.
Öpik, E. J. 1960, *Monthly Notices Roy. Astron. Soc.* **120**, 404.
——. 1963, *Advan. Astron. Astrophys.* **2**, 219.
——. 1965, *Irish Astron. J.* **7**, 92.
——. 1966, *Science* **153**, 255.
Pollack, J. B., and Sagan, C. 1967, *Smithsonian Astrophys. Obs. Special Rept.*, No. 258; 1969, *Space Sci. Rev.* **9**, 243.
Sagan, C., and Pollack, J. B. 1965, *J. Res. Nat. Bur. Std.*, Sec. D, *Radio Science* **69D**, 629.
Sagan, C., Pollack, J. B., and Goldstein, R. M. 1967, *Astron. J.* **72**, 20.
Shoemaker, E. M., Hackman, R. J., and Eggleton, R. E. 1961, *Interplanetary Correlation of Geologic Time* (U. S. Dept. Interior, Geological Survey, April).
Walker, E. H. 1967, *Icarus* **7**, 233.
Witting, J., Narin, F., and Stone, C. A. 1965, *Science* **149**, 1496.
Young, J. 1940, *J. Brit. Astron. Assoc.* **50**, 309.

APPENDIX: CRATER CATALOGUE FOR MARS FROM MARINER-4 FRAMES 7–14.

Crater number	Frame(s)	Position (cm) from south	Position (cm) from west	Diameter (km)	Class	Quality
82	7	1.9	0.9	12	3	*B*
83	7	0.9	2.1	13	3	*C*
84	7	0.6	2.9	14	3	*B*
85	7	2.0	4.0	50	4	*B*
86	7	2.7	4.1	19	2	*A*
87	7	1.3	6.4	24	3	*A*
88	7	3.0	6.0	13	3	*C*
89	7	2.3	6.5	14	2	*A*
90	7	3.1	6.8	14	4	*B*
91	7, 8	2.1, 11.2	10.2, 1.8	32, 30	3	*A*
92	7	2.3	11.5	27	4	*C*
93	7	4.8	2.4	8	2	*C*
94	7	5.8	3.2	10	2	*A*
95	7	3.7	5.9	66	4	*B*
96	7	5.1	5.2	7	2	*B*
98	7	6.6	6.4	8	2	*B*
99	7	6.0	8.0	14	3	*B*
100	7	6.0	11.4	31	4	*A*
101	7	6.3	12.7	9	2	*B*
102	7	12.2	3.0	10	1	*A*
103	7	11.5	2.8	14	3	*B*
104	7	10.7	3.3	11	3	*C*
105	7	9.8	3.4	11	3	*B*
106	7	9.7	1.4	12	3	*B*
107	7	9.6	5.1	10	3	*B*
108	7	8.8	6.6	7	3	*B*
109	7	10.8	6.4	21	3	*A*
110	7	9.9	8.9	38	4	*A*
111	7	13.9	6.9	11	4	*A*
112	7	11.0	11.1	9	1	*A*
113	7	9.9	12.0	26	2	*A*
114	7	10.3	12.8	10	2	*A*
115	7	12.2	10.9	5	2	*B*
116	7	9.2	13.5	7	2	*A*
117	7	10.7	14.3	5	2	*B*
118	7	12.0	15.1	9	2	*B*
119	7	15.5	9.7	19	1	*A*
120	7	14.3	11.9	14	4	*A*
121	7	13.3	12.4	12	2	*B*
122	7	12.9	13.3	18	3	*A*
123	7	12.8	14.7	8	2	*B*
125	7	15.0	2.6	14	2	*B*
126	7	1.5	2.0	10	1	*B*
127	8	1.9	2.7	30	4	*C*
128	8	3.0	10.9	14	3	*B*
129	8	8.3	6.4	38	3	*A*
130	8	6.1	8.1	45	3	*A*
131	8	11.0	7.6	9	1	*A*
132	8	10.5	8.7	9	2	*A*
134	8	7.6	12.6	38	4	*C*
135	8	5.3	14.0	18	4	*B*
136	8	13.8	11.6	16	4	*A*
137	8	11.9	13.3	7	2	*A*
138	8	11.2	14.0	12	3	*A*
139	8	9.6	13.9	7	2	*A*
140	8	10.2	13.2	32	4	*C*
141	8	11.2	10.2	14	3	*C*
142	8	5.9	8.6	6	2	*B*
143	8	4.0	6.7	17	4	*C*
146	9	3.7	0.7	8	2	*B*
147	9	2.9	1.5	18	3	*B*
148	9	3.8	4.5	24	4	*C*
149	9	2.4	4.6	16	3	*A*
150	9	0.8	6.7	14	3	*A*
151	9	4.5	7.3	18	1	*A*
152	9, 10	4.7, 13.8	10.7, 3.2	12, 9	3	*B, C*
153	9, 10	3.4, 12.8	10.6, 2.8	5, 6	1	*B, A*
154	9, 10	2.6, 12.0	9.9, 2.1	11, 10	1	*A*
156	9	5.8	2.4	9	2	*B*
157	9	7.3	2.5	12	3	*B*
158	9	9.6	2.1	13	3	*A*
159	9	7.2	4.5	19	4	*A*

APPENDIX (*continued*)

Crater number	Frame(s)	Position (cm) from south	Position (cm) from west	Diameter (km)	Class	Quality
160	9	7.1	5.5	18	2	*A*
161	9	9.1	5.4	27	3	*A*
162	9	10.2	6.2	9	3	*C*
163	9	9.8	6.6	6	1	*A*
164	9	8.0	6.1	7	2	*B*
165	9	6.4	8.0	7	2	*B*
166	9	8.1	8.0	33	4	*A*
167	9	8.3	8.4	11	2	*A*
168	9	7.5	10.5	24	2	*A*
169	9	7.9	12.2	7	2	*B*
170	9	8.4	12.6	22	4	*B*
171	9	10.9	2.9	10	2	*A*
172	9	12.4	2.6	27	3	*A*
173	9	12.8	2.8	6	1	*A*
174	9	11.7	8.2	27	3	*A*
175	9	11.3	9.9	5	1	*B*
176	9	15.2	10.3	52	3	*A*
177	9	12.8	12.3	15	2	*A*
178	9	5.5	1.0	10	3	*B*
179	9, 10	3.1, 12.6	14.0, 6.1	17, 25	4	*C, B*
180	9	4.8	9.5	30	4	*C*
181	9, 10	5.2, 14.4	11.5, 3.8	30, 29	4	*C, B*
182	9	6.8	12.5	13	3	*B*
184	9	9.4	10.6	6	1	*B*
185	9	12.1	6.8	6	1	*C*
186	10	2.3	2.9	9	1	*A*
187	10	4.5	5.7	33	3	*A*
188	10	2.5	10.5	34	4	*B*
189	10	−2.0	8.0	121	3	*A*
190	10	6.1	3.2	6	1	*A*
191	10	8.0	3.3	25	4	*A*
192	10	9.7	4.0	36	4	*B*
193	10	9.3	5.2	26	4	*B*
194	10	8.8	6.1	11	2	*A*
195	10	9.6	7.1	24	4	*B*
196	10	8.0	8.6	43	4	*C*
197	10	6.9	8.7	10	2	*A*
198	10	7.6	11.4	38	3	*A*
199	10	7.3	12.7	7	1	*A*
200	10	5.8	16.5	112	3	*A*
201	10	8.5	14.3	9	2	*A*
202	10	11.0	8.8	37	4	*C*
203	10	10.2	10.4	37	4	*C*
204	10	12.4	9.6	27	3	*A*
205	10	14.7	6.5	9	1	*A*
206	10	13.3	11.2	19	4	*A*
207	10	13.2	12.6	8	4	*C*
208	10	3.9	10.1	13	3	*C*
209	10	7.1	4.6	22	3	*A*
210	10	6.6	4.0	22	3	*B*
211	10	14.1	7.6	21	4	*B*
212	11	4.1	1.3	7	2	*A*
213	11	7.0	3.4	31	1	*A*
214	11	5.6	5.3	16	1	*A*
215	11	3.4	12.5	24	4	*A*
216	11	2.0	12.4	19	4	*B*
217	11	7.4	6.2	149	3	*A*
218	11	10.0	3.9	33	4	*C*
219	11	11.2	4.2	5	1	*B*
221	11	9.2	11.1	7	1	*A*
222	11	8.5	11.4	6	2	*A*
223	11	9.5	12.1	16	3	*A*
224	11	12.0	13.8	68	2	*A*
225	11	13.6	1.1	20	1	*A*
226	11	14.5	1.7	13	3	*B*
227	11	14.4	3.2	11	4	*A*
228	11	13.0	4.9	32	2	*A*
229	11	12.6	8.2	7	1	*A*
230	11	13.7	9.8	5	2	*C*
231	11	13.7	10.7	21	3	*B*
232	11	13.9	12.1	10	1	*A*
233	11	−1.2	11.9	64	3	*C*

APPENDIX (*continued*)

Crater number	Frame(s)	Position (cm) from south	Position (cm) from west	Diameter (km)	Class	Quality
234	11	4.1	6.3	17	4	*C*
235	11	2.5	6.5	32	4	*B*
236	11	1.9	5.7	18	3	*C*
237	11	3.9	4.6	39	4	*B*
238	11	8.0	4.5	15	4	*C*
239	11	14.9	2.7	12	4	*C*
240	11	7.1	12.6	22	4	*C*
241	11	8.7	13.7	24	4	*C*
242	11	5.2	1.4	6	2	*B*
243	11	4.6	1.4	5	2	*B*
244	12	2.7	0.0	65	4	*B*
245	12	7.4	2.0	12	2	*A*
246	12	8.4	3.1	6	2	*A*
247	12	7.3	5.4	8	1	*A*
248	12	8.9	7.7	11	2	*A*
249	12	3.6	13.9	13	1	*B*
250	12	4.1	14.7	18	2	*C*
251	12	6.9	13.7	19	2	*B*
253	12	12.8	13.8	31	3	*A*
254	12	12.8	9.9	41	4	*B*
255	12	13.1	2.7	31	4	*C*
257	13	12.4	0.6	13	3	*A*
258	13	13.7	2.7	13	4	*B*
259	13	12.0	4.0	19	4	*C*
260	13	13.0	7.6	37	4	*A*
261	13	11.9	9.7	28	3	*A*
262	13	11.6	9.3	15	2	*A*
263	13	13.0	11.1	11	3	*A*
264	13	15.0	11.7	9	4	*A*
265	13	7.0	8.0	11	4	*B*
266	13, 14	6.0, 15.0	11.5, 4.1	40, 42	4	*A*
267	13	7.2	14.0	10	3	*A*
268	13, 14	3.9, 12.5	12.5, 5.1	7, 5	2	*A*
269	13, 14	2.3, 10.7	12.4, 5.1	41, 45	3	*A*
270	13	13.8	11.3	11	3	*C*
271	13	14.0	5.9	9	2	*B*
272	13	10.3	9.3	23	4	*C*
273	13	5.6	12.6	14	3	*B*
274	13	6.7	5.2	21	4	*C*
275	13	5.1	6.6	20	4	*C*
276	13	3.9	8.0	36	4	*C*
277	14	4.4	6.5	21	4	*A*
278	14	3.3	10.2	33	4	*A*
279	14	1.4	11.7	12	4	*B*
280	14	6.9	6.2	18	4	*A*
281	14	11.4	9.2	7	1	*A*
282	14	8.4	10.2	86	4	*A*
283	14	9.8	12.4	12	4	*B*
284	14	10.9	14.4	41	2	*A*
285	14	14.6	11.3	22	4	*C*
286	14	12.5	12.2	43	4	*B*
287	14	6.9	11.4	19	4	*C*
288	14	7.4	9.6	19	4	*C*
289	14	8.4	9.0	22	4	*C*
290	14	4.4	4.6	58	4	*C*
291	14	2.5	6.0	8	1	*A*
292	14	1.8	6.8	9	1	*A*